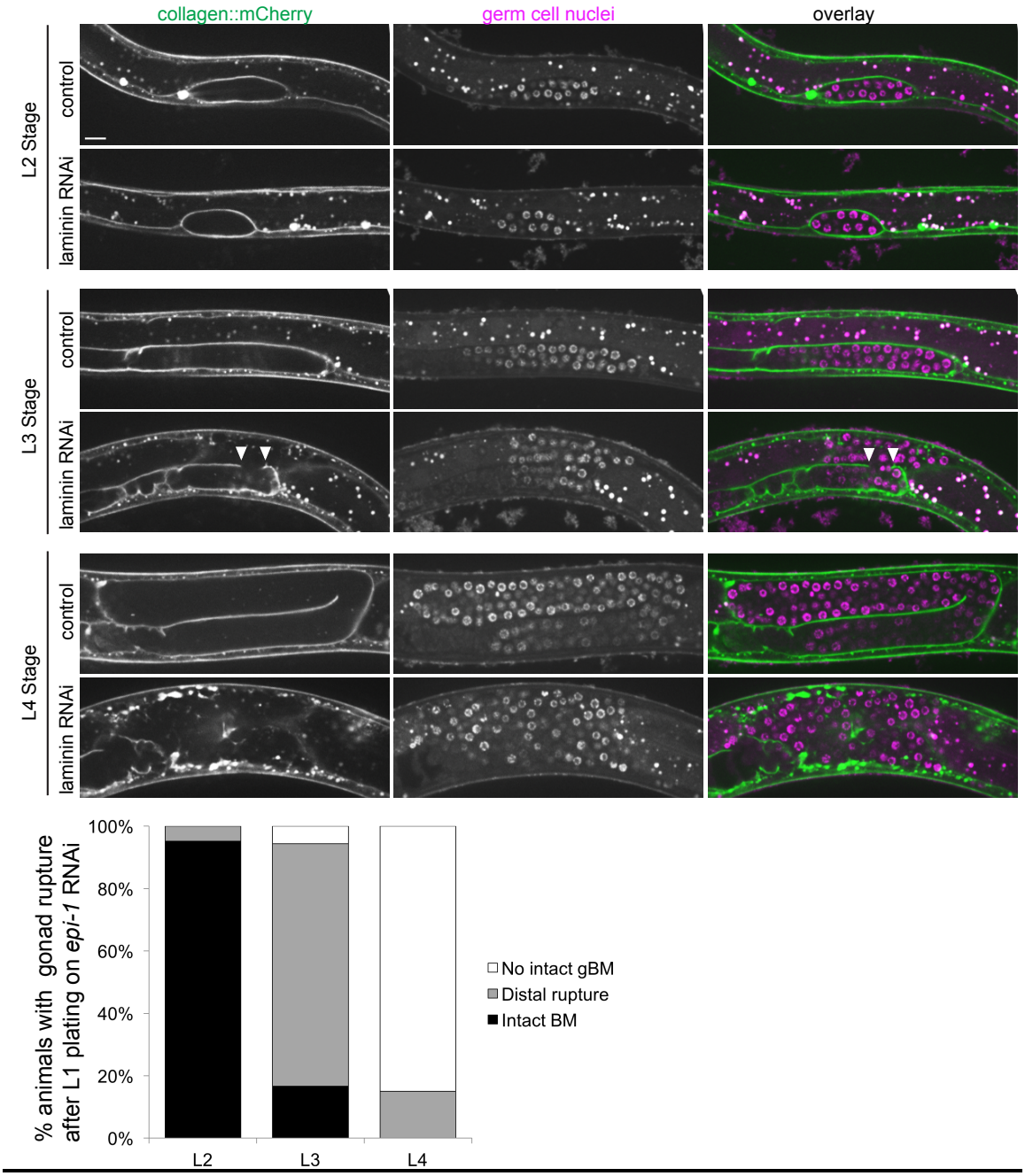

Figure S1. Gonadal basement membrane ruptures allow germ cell escape in laminin RNAi-treated animals. Related to Figure 1.

Control animals (top row each stage) and animals reared on *epi-1*(laminin) RNAi from the L1 larval stage (bottom row of each stage) with basement membranes marked with *emb-9p::emb-9::mCherry* (left, tagged collagen); germ cells marked with *pie-1p::H2B::GFP* (center). Overlay right. RNAi-treated animals experience gonadal basement membrane ruptures rarely in the L2 stage (n = 1/21), and primarily during the L3 (n = 15/18) and L4 (n = 20/20) stages (and Figure 1B); gonad rupture in control animals raised on the empty RNAi vector L4440 was not observed (n = 0/20 for L2 and L3, n = 0/10 for L4). Arrowheads indicate an example of a “distal rupture” of the basement membrane. Single optical sections through the middle of the gonad are shown. Scale bar is 10 µm. Graph shows quantification of gonadal rupture in *epi-1*-RNAi treated animals for the aforementioned datasets.

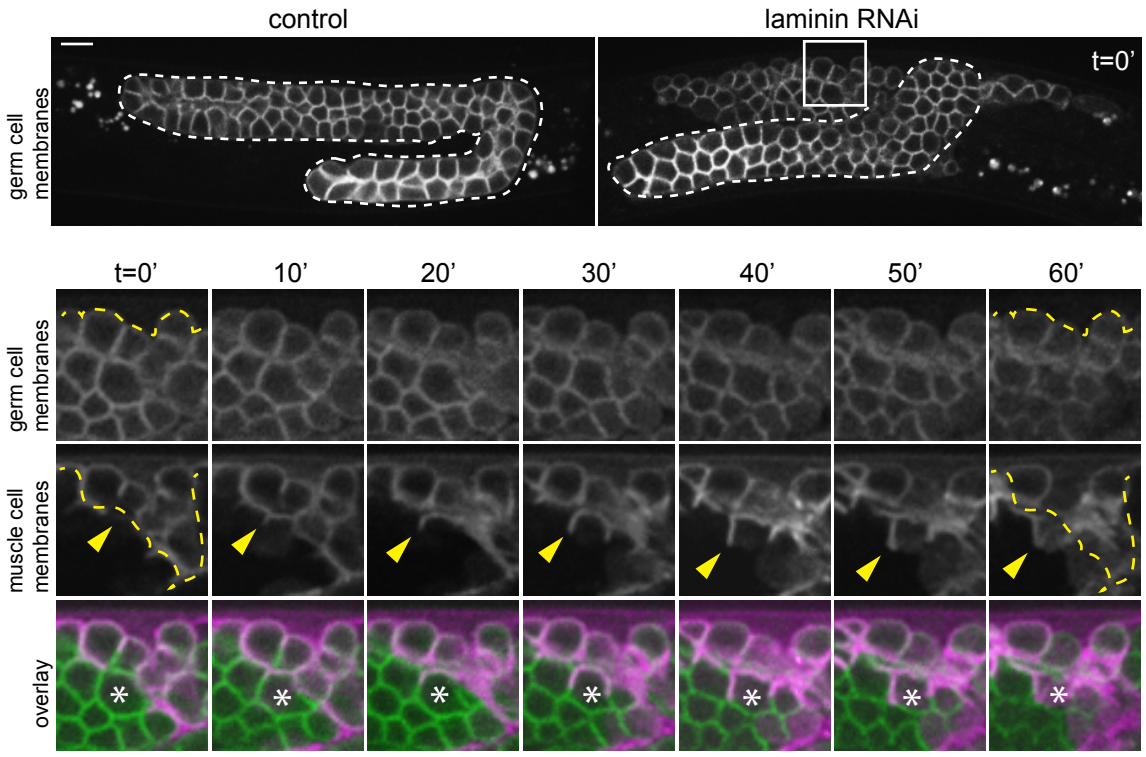

Figure S2. Escaped germ cells are not invasive, but muscle cells are protrusive. Related to Figure 1 and Video S1. Germ cells (*mex-5p::GFP:: PLCδ^{PH})* escaped from the gonad (dashed white line) following *epi-1* RNAi treatment (right top), but not control (left top). Breaks in white dashed line indicate ruptures in the basement membrane. The box indicates the magnified region. Over time (bottom panels), escaped germ cell membranes (green in overlay) were not protrusive, while muscle cell membranes (magenta in overlay, *myo-3p::mCherry::PLCδ^{PH}*) extended dynamic protrusions (n = 9/9 animals, 60-minute time-lapse movies). Yellow dashed line indicates starting boundary of germ cells (top row) and muscle cells (middle row) both in time t = 0 ' and the same line superimposed over t = 60 ' to show change over time. Arrowhead indicates a single growing muscle protrusion over time. Asterisk in overlay (bottom row) indicates a single germ cell nucleus becoming enwrapped over time. Same individual shown in Video S1. Figure 1C and 1D shows time-lapse with germ cell nuclei instead of membranes labeled. Animals were imaged at the L4 larval stage following laminin RNAi treatment at the L2 stage. Single confocal z-slices are shown. Scale bar is 10 μm.

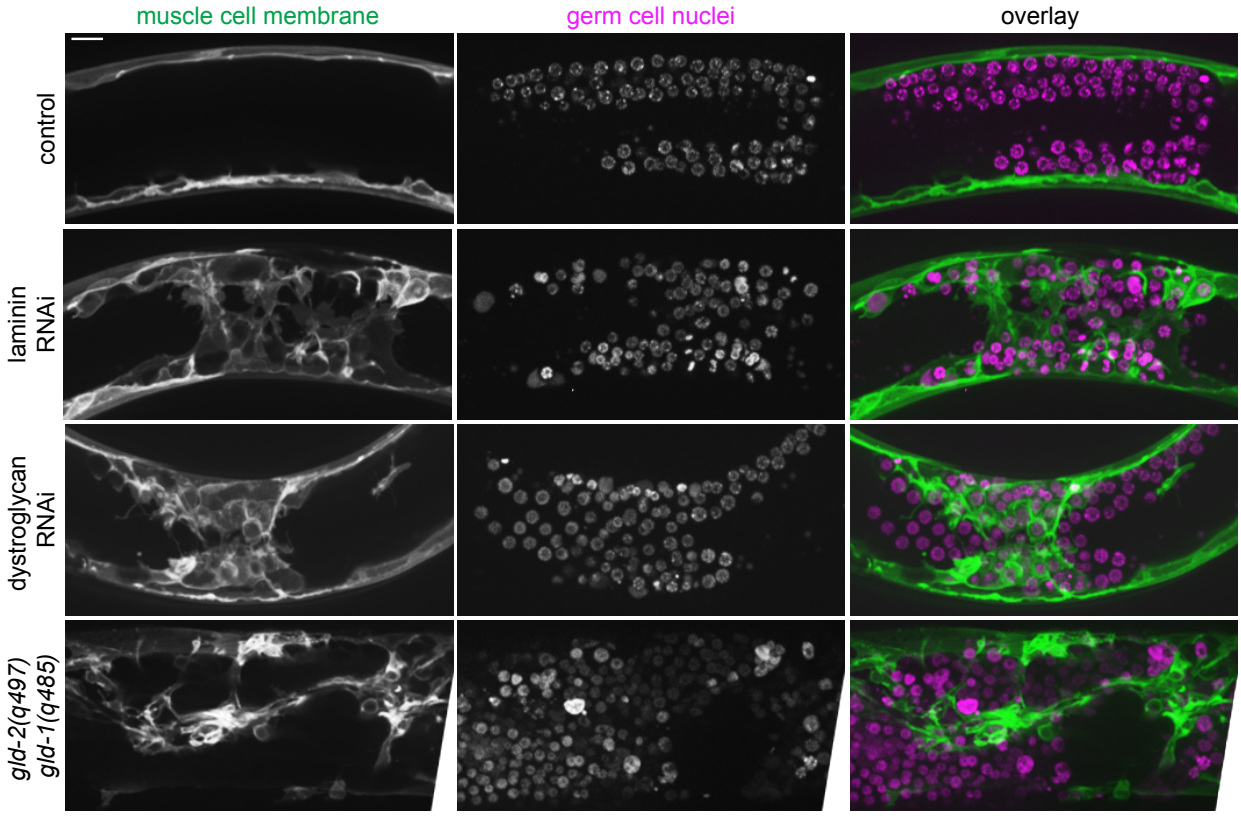

Figure S3. Muscle cells enwrap germ cells in multiple genetic backgrounds that cause gonadal basement membrane rupture. Related to Figure 1.
Muscle cells (left, *myo-3p::GFP::CAAX*) enwrap escaped germ cells (center, *mex-5p::H2B::mCherry*) following basement membrane ruptures caused by multiple treatments. No cases of gonadal basement membrane rupture were observed in animals fed empty RNAi vector L4440, while RNAi knockdown of *epi-1/*laminin (second row) and *dgn-1/*dystroglycan (third row, dataset also includes *myo-3p::mCherry*-marked worms), as well as germline hyperproliferation caused by loss of germline meiotic entry regulators GLD-2 and GLD-1 (bottom row) caused gonadal rupture. Animals with gonadal ruptures were scored at the L4 to adult stages. The control and *epi-1* RNAi dataset also appear in Figure 1. All images are 5 µm core projections of confocal z-stacks. Scale bar is 10 µm.

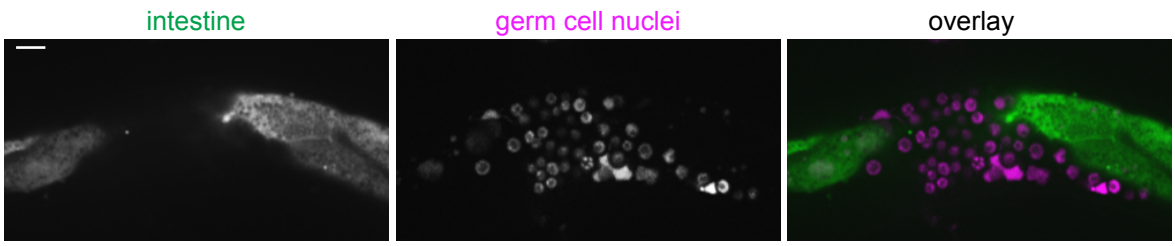

Figure S4. Escaped germ cells do not become enwrapped by intestine. Related to Figure 2.
Escaped germ cells (center, *mex5p::H2B::mCherry*) did not embed in the intestine (left, *ges-1p::GFP*) in *epi-1*/laminin RNAi-treated animals (n = 0/11). Germ cells do embed in muscle (Figure 1C) and hypodermis (Figure 2A). A single confocal z-slice of each channel (left, middle) and overlay (right) are shown. Scale bar is 10 µm.

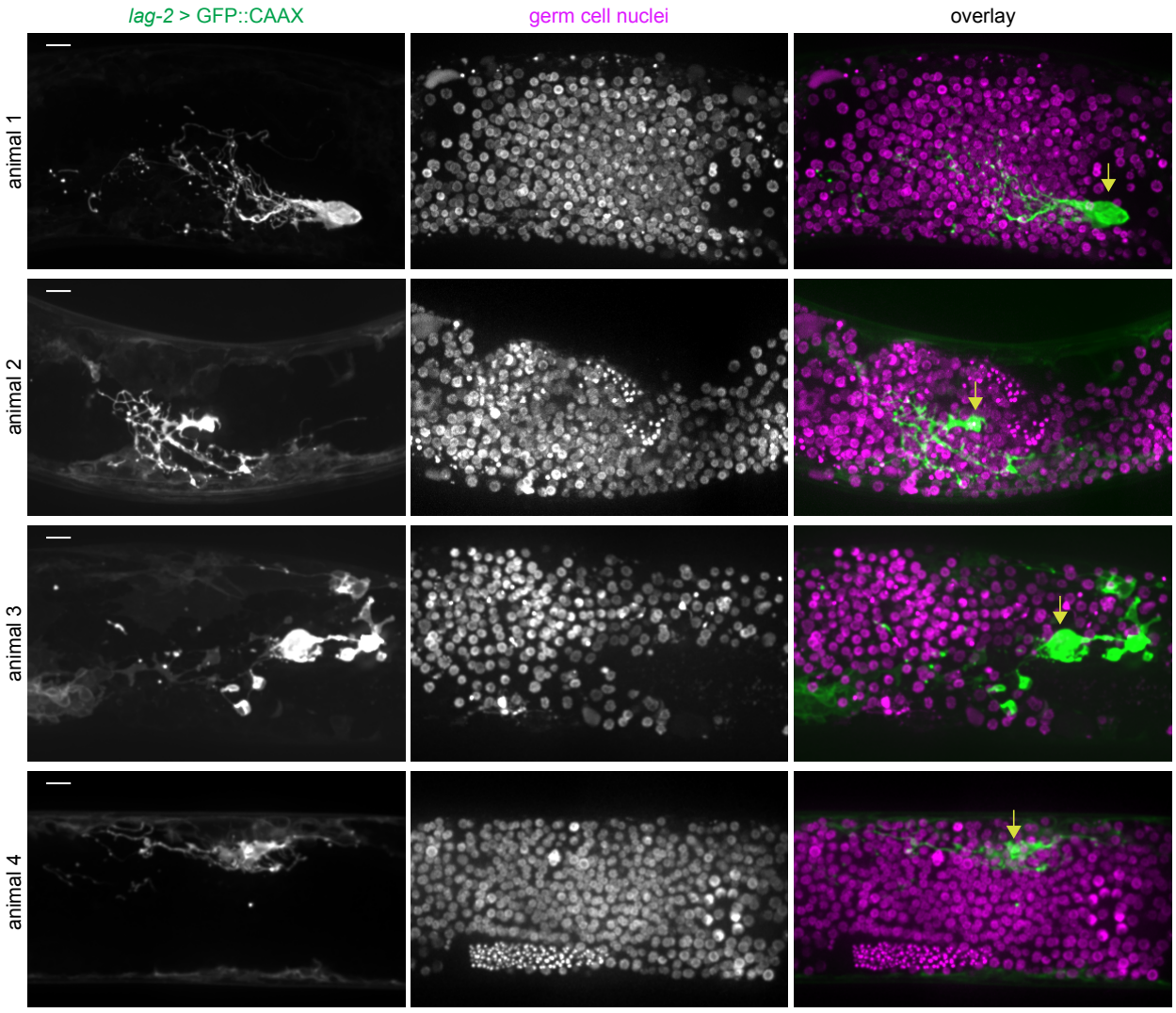

Figure S5. DTC protrusions persist after gonad rupture. Related to Figure 3.
Four animals expressing *lag-2p::GFP::CAAX* (left) with the DTC (arrow in overlay, right) sending projections in all directions enwrapping a robust germ cell population (center, *mex-5p::H2B::mCherry*) after *epi-1* RNAi treatment. Maximum intensity z-projections through a depth encompassing the extent of the DTC processes are shown. Animals 1-3 imaged 48 h after mock ablation. Animal 4 imaged 24 hours after mock ablation. A narrower projection from animal 1 appears in Figure 3. Scale bars are 10 μm.

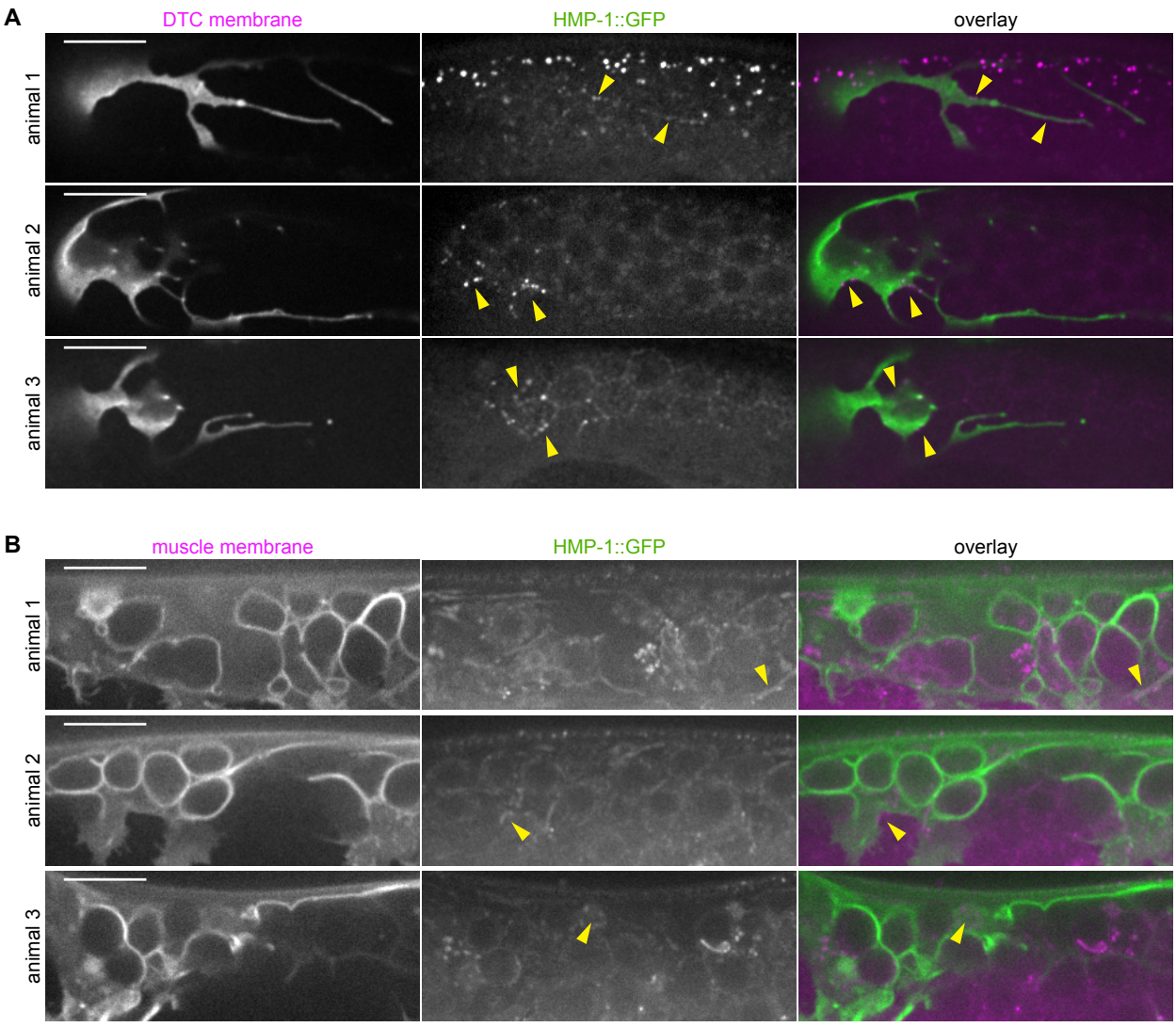

Figure S6. HMP-1 is expressed in the DTC and in muscle. Related to Figure 5.
Because only 3/6 isoforms of HMP-1 are tagged with GFP, and because the tagged protein is expressed in germ cells (center, and Figure 5), protein localization in confocal z-projections (Figure 5) can be difficult to see. Single confocal z-sections are shown here with HMP-1::GFP clearly visible in the DTC (A), germ cells (A, animal 3), and less strongly in muscle (B). Arrowheads indicate selected HMP-1::GFP localization in focal tissues. All scale bars are 10 µm.

Sequence	Name	% defect	Description
F02E9.5		100	ortholog of human OSER1
F02E9.7		100	ortholog of human ACP5
K04G2.7		100	enriched in germline
T22A3.8, C43H8.3	*lam-3*	100	orthologous to human laminin alpha2; sterile worms noted on plate
D1081.7		90	enriched in germline
W02B9.1	*hmr-1*	90	E-cadherin ortholog
B0205.4		100	homolog of the human gene FUT1
C03C11.1		100	enriched in germline
C03D6.5	*asfl-1*	100	histone chaperone
C03D6.8	*rpl-24.2*	100	ribosomal subunit L24 paralog; homolgous mammalian L30 and yeast Rlp24
C43H8.1	*arch-1*	100	ortholog of human ZBTB8OS
C47F8.7		100	unknown
C54C8.11	*gly-15*	100	similar to 2/I N-acetylglucosaminyltransferase
C54C8.9	*nlp-39*	100	unknown
D1081.6		100	ortholog of human LY6D
F02E9.1		100	divergent ortholog of S. cerevisiae VMA22
F02E9.4	*sin-3*	100	histone deacetylase subunit
F10D11.2		100	unknown
F10D11.5		100	unknown
F10D11.6		100	ortholog of members of the human BPIF family including BPI
F26E4.5		100	SH2 domain-containing tyrosine kinase
F35E2.3		100	enriched in germline
F36D1.4		100	unknown
F41D3.2	*oac-26*	100	predicted to have transferase activity
F46A8.9		100	pseudogene
K02B12.6		100	unknown
K07A1.7	*cri-1*	100	ortholog of human HECA
M04C7.2		100	transposon
Y47H9C.12		100	unknown
Y52B11A.7	*mltn-2*	100	mlt-10 related
Y53C10A.10.1		100	enriched in germline
Y95D11A.10		100	contains a MIF4G domain found in proteins involved in RNA metabolism
C25A1.15		90	unknown
K02B12.7		90	ortholog of human ARFGAP1
Y67A6A.2	*nhr-62*	90	predicted zinc-binding steroid hormone receptor DNA-binding transcription factor

N≥10 in each trial; genes in white cells detected in muscle transcriptome

Table S1. RNAi causing DTC defect in given percentage of animals. Related to Figure 4 and Results section “DTC adhesion to germ cells is mediated by E-cadherin and L1CAM”.